Adv. Nat. Sci.: Nanosci. Nanotechnol. **12** (2021) 015001 (9pp) https://doi.org/10.1088/2043-6254/abdfc1

Nanoparticles synthesised from *Caesalpinia spinosa*: assessment of the antifungal effects in protective systems

Erasmo Gámez-Espinosa[1], **Cecilia Deyá**[1,2], **Marta Cabello**[3,4] **and Natalia Bellotti**[1,4]

[1] Centro de Investigación y Desarrollo en Tecnología de Pinturas (CONICET-CICBA-Ing.-UNLP), Buenos Aires, Argentina
[2] Facultad de Ingeniería. Universidad Nacional de La Plata, Buenos Aires, Argentina
[3] Instituto de Botánica 'Carlos Spegazzini' (CICPBA-UNLP),Buenos Aires, Argentina
[4] Facultad de Ciencias Naturales y Museo. Universidad Nacional de La Plata, Buenos Aires, Argentina

E-mail: e.gamez@cidepint.ing.unlp.edu.ar and n.bellotti@cidepint.ing.unlp.edu.ar

Received 29 June 2020
Accepted for publication 26 September 2020
Published 4 February 2021

Abstract

Green chemistry is the preferred approach for the synthesis of metal and metal oxide nanoparticles due to its environmental friendliness, feasibility, and safety to human health when compared with other chemical or physical methods. *Caesalpinia spinosa* is a promising resource to be applied in the green synthesis of metallic nanoparticles due to the high amount of polyphenols. The aim of the present research was to obtain an antifungal coating functionalised with nanoparticles synthesised from *C. spinosa* tannin and aqueous solutions of metallic (silver and copper) salts to control biodeterioration of acrylic paints and bricks. Green synthesised NPs were characterised by UV-vis spectroscopy, transmission electron microscopy (TEM), Fourier transformed infrared spectroscopy (FTIR), scanning electron microscopy (SEM) and energy dispersive x-ray spectroscopy (EDS). The silver nanoparticles with average size of 12 nm and obtained from a 500 ppm aqueous solution of *C. spinosa* tannin inhibited the growth of *Aspergillus niger*, *Penicillium commune* and *Lasiodiplodia theobromae*. These strains were previously isolated from a biodeteriorated facade. Functionalised coating obtained with silver nanoparticles synthesised from *C. spinosa* tannin is reported for the first time as antifungal protective system of acrylic paints and bricks.

Keywords: Green nanotechnology, biogenic nanoparticles, tara tannin, protective coating, fungi
Classification numbers: 2.04, 2.05, 4.02, 5.08

1. Introduction

The filamentous fungi promote biodeterioration processes that cause aesthetic, physical and chemical damage to materials due to their metabolic activity. As a consequence, this causes economic losses and health problems for exposed people [1, 2]. In this sense, ceramic materials exposed to outdoor conditions are often affected by fungal deterioration. Porosity and surface roughness play a major role in bioreceptivity to colonisation [3]. The use of antifungal functionalised coating with nanoparticles (NPs) to control biodeterioration is being intensively studied [4].

Green nanotechnology provides tools to obtain NPs using biological systems and preventing any associated toxicity [5, 6]. While a large number of toxic chemicals and extreme environments are employed in the physicochemical production of NPs, green methods employ biological sources and water as solvent [7]. Biogenesis of metal NPs draws significant attention due to environment eco-friendly and sustainable methods [8]. Plants are the most preferred source of all macro- and microscopic entities used for the green synthesis (phytogenic synthesis) of NPs due to the simplicity, nontoxicity, and easy availability of raw materials [9]. In addition, phytochemicals such as polyphenols, alkaloids,

steroids, phenolics, terpenoids, and saponins exhibit natural biological properties [10, 11].

Polyphenols, the major constituents of tannins, are important phytochemicals that form part of the plant defence system and are mainly found in their fruits, seeds, flowers, and barks [12–14]. The unique chemical properties of tannin have led to its wide use as a food colorant, antioxidant, waste water treatment agent, metal adsorbent, bio-based material and in leather tanning applications [15, 16]. Compared with metals and synthetic organic tanning agents, vegetable tannin has the advantages of being renewable, environmentally friendly, and safe to use [17]. *Caesalpinia spinosa*, known as 'tara' tree, is a small thorny tree frequently found in arid areas of South America and is characterised for its fruit pods which contain a high amount of polyphenols greater than 40%. [18]. Principal components of 'tara' tannin (TT) are hydrolysable polyphenols based on a galloylated quinic acid structure [19]. Polyphenols as those present in TT possess antioxidant properties which could be attributed to their ability to donate hydrogen atoms, electrons and be strong chelating agents [20, 21]. This turns out to be promising to the bio-reduction of metallic ions to obtain NPs with antimicrobial activity [22].

The antifungal activity of the NPs is attributed largely to the interaction of these with thiol or amino groups present in biomolecules. On the other hand, metal NPs can release ions that would affect proteins and nucleic acids at the structural level, and also generate highly reactive oxygenated chemical species as widely reported [23, 24]. Therefore, the aim of the present research was, primarily, to assess the use of tannin from *Caesalpinia spinosa* in the synthesis of antifungal NPs using silver and copper salt aqueous solutions. Then, the most active nano-additive was applied in functionalised coatings to control the biodeterioration of acrylic paints and bricks.

2. Materials and methods

2.1. Green synthesis and characterisation of nanoparticles

The nanoparticles were obtained from aqueous solutions of $AgNO_3$ and $Cu(NO_3)_2.3H_2O$ to which the TT solution was added in constant agitation during 30 min. The final concentration of the salts in the synthesis system was 10^{-2} M in both cases. Three concentrations of TT were used: 500, 1000 and 2000 ppm. The TT (Indunor) used was a commercial one. This process was done at 60 °C and the pH was adjusted to 7 by a NH_4OH solution [25]. The stability of the NPs suspensions over time was evaluated by UV-vis spectroscopy carried out at different times: 24 h, 1 month and 3 months. The equipment used was a spectrophotometer UV SP2000. Transmission electron microscopy (TEM) was applied to confirm the obtainment of the nanoparticles, observe their morphology and particle size. The equipment used was a JEOL 100 CXII at an acceleration voltage of 100 KV. Scanning electron microscopy (SEM) and energy dispersive x-ray spectroscopy (EDS) mapping were made to the purified NPs. The observations and analyses were carried out in low vacuum, the equipment used was a FEI Quanta 200 Philips. The NPs were purified by successive washes using a microcentrifuge DLAB D3024R at 15000 rpm during 20 min at 20 °C [25]. Fourier transformed infrared spectroscopy (FTIR) spectra of the purified NPs were obtained using the KBr disk method by a Perkin-Elmer Spectrum One spectrometer. The analysis of the spectra was carried out using the KnowItAll® Informatics System program, Version: 10.0.18362.

2.2. Fungal strains selected

The strains selected for this study were *Aspergillus niger* MN371276, *Penicillium commune* MN371392 and *Lasiodiplodia theobromae* MN371283. They were isolated from biodeteriorated facade of the Cathedral of La Plata city (34° 55′S, 57°57′O) in a previous research work. All the strains were identified from the polyphasic taxonomy, firstly based on the morphology of the somatic and reproductive structures [26]. Moreover, taxonomic identification from morphological structures was confirmed by molecular techniques. The amplification and sequencing of the selected regions using ITS1 and ITS4 primers were carried out by Macrogen company [27]. Macrogen sequencing service is provided by 3730XL DNA analyser (AB, USA) and BigDye v3.1 (AB, USA). In case of eukaryote, after rRNA sequencing, it is possible to find out the similarity of customer's microorganism with microorganism in National Center for Biotechnology Information (NCBI).

2.3. Antifungal activities of nanoparticles

The antifungal activity of the NPs suspensions was determined by two tests: agar diffusion method (Kirby-Bauer) and fungal growth inhibition in macrodilution assay [28]. In the case of Kirby-Bauer test, 6 mm paper discs embedded with the NPs suspensions were placed on 15 ml of inoculated malt agar extract (MEA) medium. Physiological solution was used as negative control while the positive control was a quaternary ammonium salt ($[CH_3(CH_2)_{15}N(CH_3)_3]Br$) solution. The incubation period was 48 h and the temperature was regulated at 28 °C.

The diameter (D) of the inhibition zone around each disc was registered using a digital caliber. Therefore, a tested sample was considered active when D was greater than or equal to 6 mm, and not active when D was less than 6 mm. To the macrodilution method, fungal growth was determined through the measurement of the colony diameters. Suspension of NPs was added in Petri dishes with MEA, so that the final dilutions have concentrations of 10, 50 and 167 μg ml^{-1}. As a control, NPs-free (0 μg ml^{-1}) Petri dishes with MEA were used. Subsequently, the plates were inoculated in the center with 20 μl spore suspension at 10^5 spores/ml and incubated for 7 days at 28 °C. The test was carried out in triplicate.

2.4. Formulation, preparation and characterisation of nano functionalised coatings

NPs functionalised sol-gel coating was prepared to be applied in the protection of acrylic paints and bricks for outdoor environments. The acrylic paint was specially prepared to the

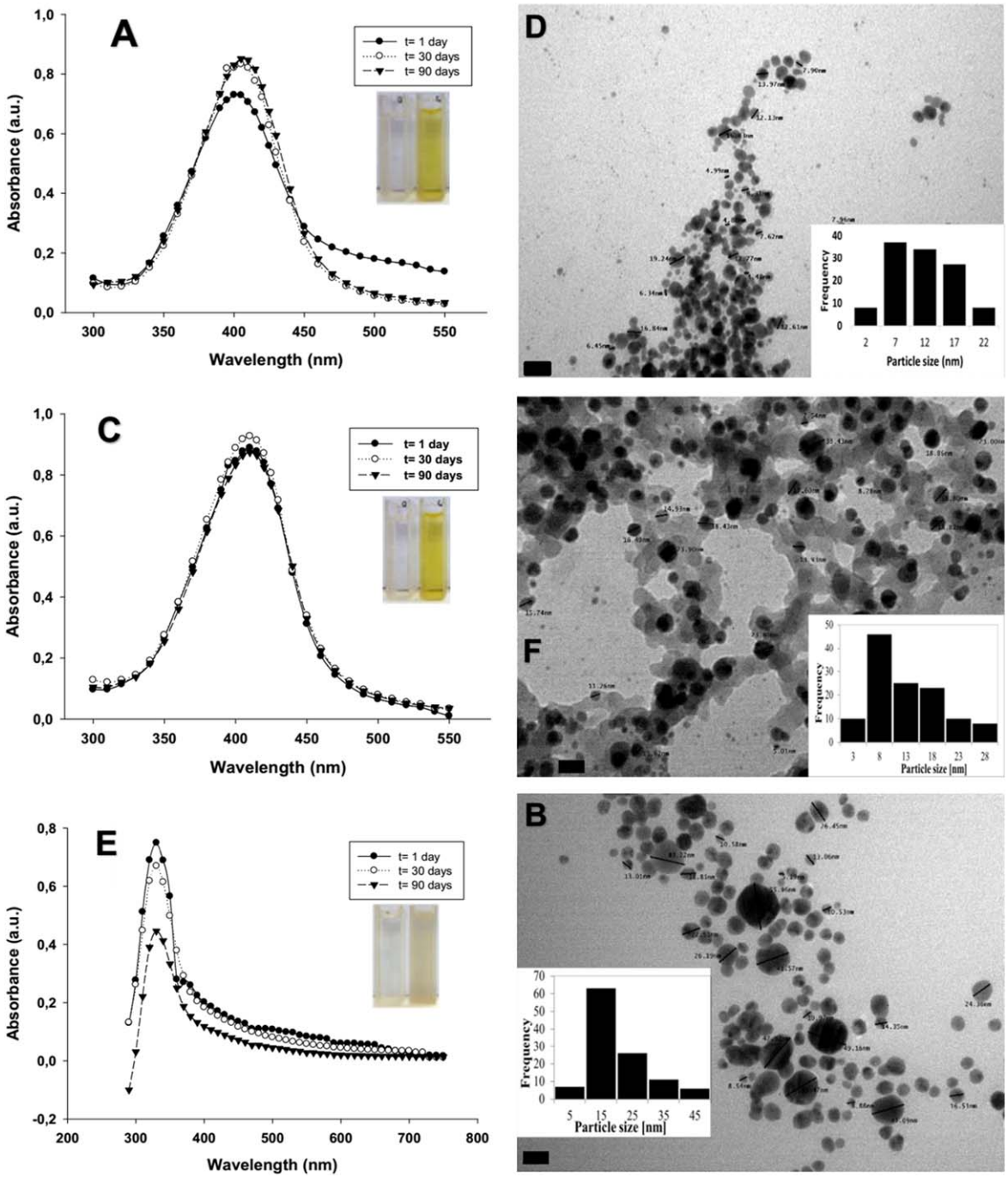

Figure 1. UV-vis spectra, TEM micrographs and histograms from size distribution analysis of NPs obtained from TT: (A) and (B) Ag1NPs, (C) and (D) Ag5NPs, (E) and (F) CuNPs. Magnification: 270000× and scale bar: 20 nm in (B), (D) and (F).

present research while the bricks were commercially obtained. The paint was prepared in a high speed disperser with the following composition: 26.2% acrylic resin, 10.0% TiO_2, 21.9% $CaCO_3$ (natural), 1.9% $CaCO_3$ (precipitated), 1.6% additives (antifoaming, cellulosic thickener, dispersants and surfactants) and 38.4% distilled water (DW) (% by weight). Finally, the paint was applied in glass slides to be treated then by the sol-gel coating.

To the sol-gel coatings, 3-Aminopropyl triethoxysilane (AMEO) (Camsi-X, used as supplied) was used as silane precursor and added in a concentration of 2% (v/v). The precursor was added to the system in a ratio of 0.9 ml per each ml of ethanol together with 0.06 ml ml^{-1} of NPs suspensions and 2% of distilled water (DW). The pH was previously adjusted to 4 with HNO_3. DW was used as control in replacement of NPs suspensions. Hydrolysis time was one hour, after which, studied samples (bricks of 4 cm^3 and slide glasses with acrylic paint of 2.5 cm^2) were treated by immersion for 90 s in the prepared solutions and then drying at room temperature for two weeks [29]. After this, the antifungal activity of the acrylic paint and brick coated samples was evaluated.

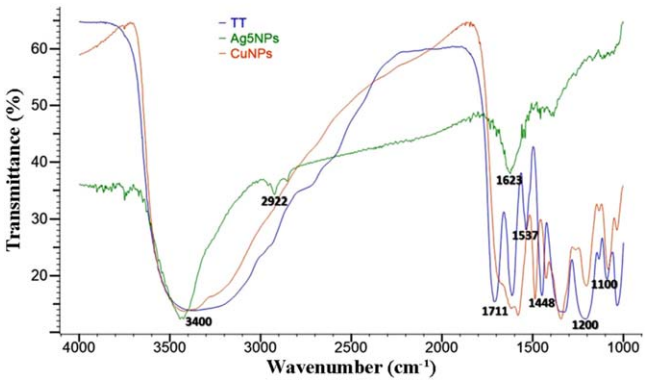

Figure 2. FTIR spectra of *C. spinosa* tannin (TT) and the NPs obtained.

The silane coatings were characterised by SEM, EDS and x-ray mapping. In addition to this, contact angles were determined [30] using the drop method with water as solvent on the surface of the treated samples of brick or acrylic paint. Photographic records and the contact angles were obtained by digital Gaosuo microscope and the corresponding software of the same device. The measurements were performed in triplicate.

2.5. Fungal resistance test of nano functionalised coatings

The antifungal activity of the samples, bricks and acrylic paint films with the NPs-functionalised coatings was evaluated using ASTM 5590 standard. The samples were inoculated with a same volume of spore suspension and placed in Petri dishes with minimum mineral agar (MMA). The incubation period was 30 days at 28 °C. The fungal growth observed in the samples was classified according to the percentage of the covered area (%). Sample without growth (0%), growth in traces (below 10%), light growth (10%–30%), moderate growth (30%–60%) and heavy growth (60%–100%) were evaluated as 0, 1, 2, 3, and 4 respectively. Finally, the samples were observed by stereoscopic microscope (Leica S8 APO) and SEM (Philips FEI Quanta 200). The working conditions were high vacuum (10^{-6} Torr) [31]. The test was performed in triplicate.

2.6. Statistical analysis

Statistical analysis of the measurement of the colony diameter was performed with the RStudio 1.1.463® program. The probability distribution was analysed with normal distribution test. A one-way ANOVA was performed and subsequently Tukey's test was applied. The factor included was nanoparticle concentration. The tests used were applied using the multcomp package.

3. Results and discussion

3.1. Green synthesis and characterisation of nanoparticles

It was possible to obtain stable NPs with the proposed biosynthesis method. Figure 1 provides the UV-vis spectra, TEM micrographs and histograms from size distribution of the stable NPs in solution, obtained from $AgNO_3$ and TT at 1000 and 500 ppm, Ag1NPs and Ag5NPs, respectively. The products obtained with 2000 ppm of TT and the Ag salt solution were unstable and precipitated before 24 h. On the other hand, with the $Cu(NO_3)_2.3H_2O$ solution, NPs could only be obtained when the TT concentration was 2000 ppm (CuNPs) which was corroborated by UV-vis spectroscopy. Figures 1(A) and (C) show the UV-vis spectra of Ag1NPs and Ag5NPs, respectively. The spectra depicted a maximum peak observed between 400 and 410 nm that is maintained over time, but increases in intensity for Ag5NPs. These absorption bands are characteristic of nanoparticles and correspond to the surface plasmon resonance (SPR). In addition, the sizes of both Ag1NPs and Ag5NPs are quasi-spherical (figures 1(B) and (D)). However, Ag1NPs have the higher frequency at sizes larger than 10 nm and an average size of 20 nm. Meanwhile Ag5NPs showed higher frequency for the lowest sizes with an average size of 12 nm. In the case of CuNPs, an absorption band with a maximum at about 350 nm can be seen in figure 1(E). This band would correspond to the cuprous oxide SPR [32], remained stable over time, but on 90th day a decrease in the intensity was observed. CuNPs are also quasi-spherical and the average size registered was of 17 nm (figure 1(F)).

Other methods for the characterisation of the NPs are SEM, EDS and FTIR [33]. Figure 1 of supplementary material shows SEM micrographs, EDS spectra and NPs mappings. In this sense, Ag1NPs and Ag5NPs present a compact arrangement (figures 1(A) and (D)) and uniform distribution which is observed in the mapping (figures 1(B) and (E)). The uniform distribution of the nanoparticles may depend on several parameters, for example the arrangement of the particles in the sample preparation, their morphological uniformity, types of electrons (secondary electron detector) and the working conditions (high vacuum). Likewise, EDS spectra of both NPs showed an Ag resolute peak at 3 keV (figures 1(C) and (F)), which clearly confirms the obtainment of the AgNPs and reaffirms the results described by UV-vis spectroscopy. CuNPs also have compact arrangement (figure 1(G)) similar to AgNPs and a uniform distribution with the difference in the appearance of a strong oxygen signal which would be corroborating the presence of copper oxide (figure 1(H)). In addition, figure 2 shows a Cu peak approximately at 0.9 keV, confirming the obtainment of cuprous oxide NPs.

Figure 2 depicted IR spectra of the purified NPs obtained from TT and the TT itself. The three products show a broad band between 3600–3200 cm^{-1} corresponding to the stretching of the O-H group (intra-molecular H bonds, single bridge) present in polyphenols. Increases in the strength of H-bonds are accompanied by shifts to lower frequencies of

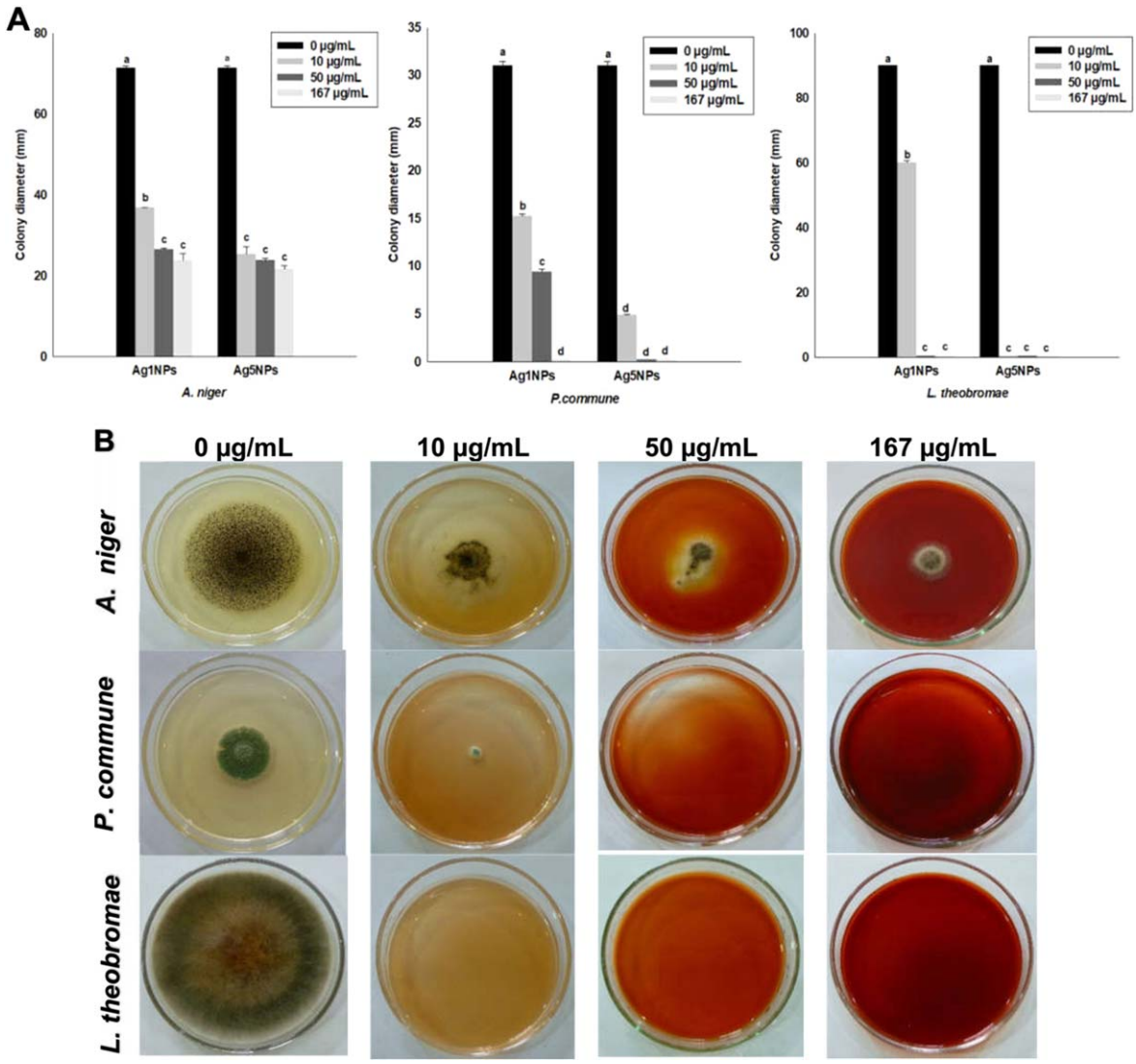

Figure 3. Effect of NPs on the colony diameter. (A) Colony diameter measurements, different letters on bars indicate statistically significant difference ($\rho \leqslant 0.05$) and for Tukey test. (B) Fungal growth in Petri dish with MEA and Ag5NPs, $t = 7$ days, $T = 28$ °C.

the absorption bands due to O-H stretching vibration as seen in the case of TT [34]. The peak at 2922 cm^{-1} corresponding to ring CH_2 symmetric stretching is more defined in the case of the AgNPs. The TT spectrum presents a defined and strong peak at 1711 cm^{-1} which corresponds to the stretching of the carbonyl –C=O groups present in gallotannins. The disappearance of this peak in the spectra of both NPs could be related with the reduction mechanisms. In this sense, electron donation from carbonil groups would be related to the change in its stretching frequency [12]. The three spectra have the presence of peaks between 1623 and 1600 cm^{-1} corresponding to carboxyl groups in this type of polyphenols. Two peaks at 1537 and 1448 cm^{-1} can be observed in TT spectrum that correspond to stretching of C=C bond of the aromatic ring [35]. These peaks were displaced towards to lower wavenumbers in the case of the NPs. In all cases, the peaks at about 1200 and 1100 cm^{-1} correspond to the phenolic C–O bonds vibration [12]. The FTIR spectra proved that the gallotannin is strongly associated with the purified NPs and therefore with the synthesis mechanism. Taking into account this, polyphenols present in the TT would reduce metal ions (M^+ to M°) acting as green reducing and stabilising agent.

3.2. Antifungal activities of nanoparticles

Agar diffusion assay showed that only Ag1NPs and Ag5NPs suspensions have antifungal activity on all the strains studied. For this reason, only these NPs suspensions were used in the macrodilution assay. Figure 3 presents the effect of NPs on the mycelial growth of the studied strains. Furthermore, figure 3(A) shows that there are statistically significant differences ($\rho \leqslant 0.05$) between the colony diameter values of the *A. niger* when the concentration of Ag1NPs and Ag5NPs was 10 $\mu g\,ml^{-1}$. In the case of *P. commune* and *L. theobromae*, no statistically significant differences were observed between the concentrations of Ag5NPs, indicating the same biological effect of these NPs, regardless of the concentration used. Thus, greater antifungal activity of Ag5NPs with respect to Ag1NPs is demonstrated. Although no total growth inhibition is observed in *A. niger*, the relationship between the

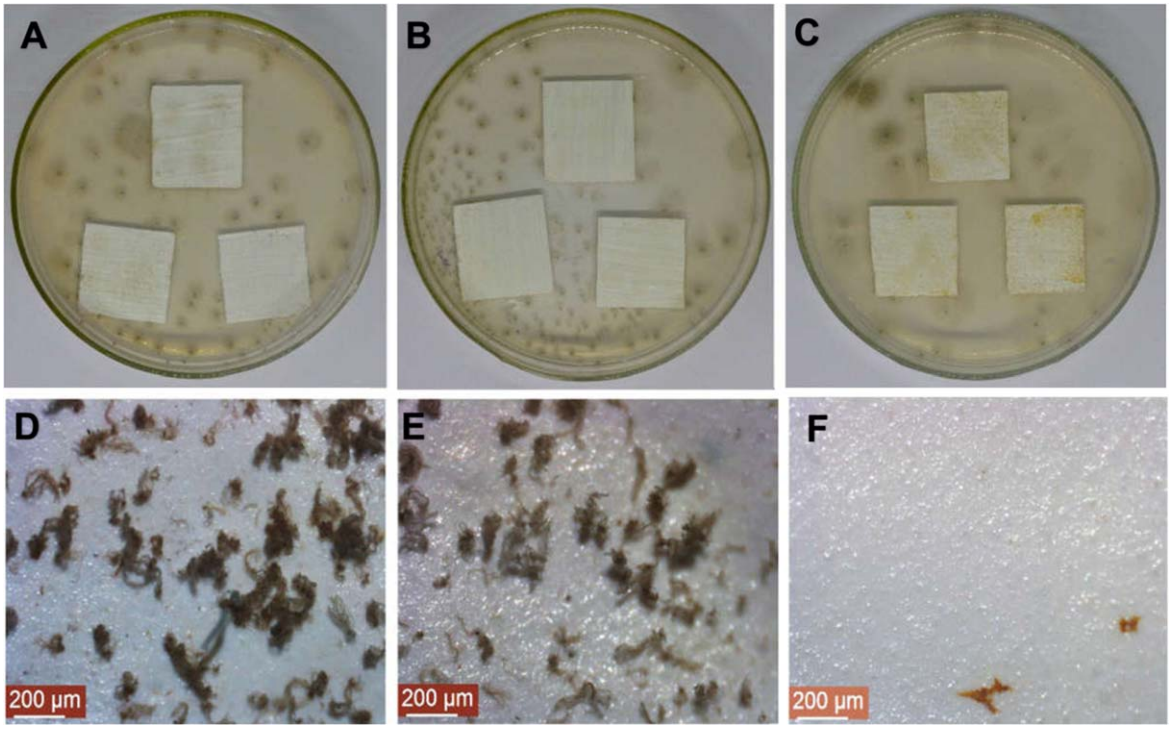

Figure 4. Fungal resistance test against *P. commune*, samples: (A) and (D) control (paint sol-gel free coating), (B) and (E) sol-gel coating over the paint, (C) and (F) sol-gel coating + Ag5NPs over the paint. (D)–(F) were obtained from stereoscopic microscope (80×), $t = 30$ days.

Table 1. Fungal growth rating according to the area covered.

Sample	*A. niger*	*P. commune*	*L. theobromae*
Paint sol-gel free coating	4	3	4
Sol-gel coating over the paint	4	3	3
Sol-gel coating + Ag5NPs over the paint	2	0	0
Brick free of sol-gel coating	4	4	4
Brick with sol-gel coating	3	3	3
Brick with sol-gel coating + Ag5NPs	0	1	0

colony diameter and the concentration of Ag5Nps is inversely proportional. The total growth inhibition was obtained against *P. commune* and *L. theobromae* at 50 and 10 μg ml^{-1}, respectively (figure 3(B)). Other authors have also reported the antifungal activity of AgNPs. For instance, Odeniyi *et al* [21] obtained AgNPs from green reducers that had antifungal activity against *A. niger* and Valsalam *et al* [22] described AgNps green synthesised from the leaf extract of *Tropaeolum majus* and their activity against *Penicilium* sp. According to the scientific literature, a possible mechanism of antifungal activity is based on the internalisation of AgNPs by the apical end of the growing hypha. Once the NPs are in the intracellular medium, their strong interaction with nucleophiles such as amino and thiol groups causes the inactivation of some enzymes and affects processes such as nutrition and cellular respiration. Silver ions can cause denaturation of biomolecules (e.g. nucleic acids, enzymes and proteins), which affects the fungal cell viability [36].

3.3. Formulation, preparation and characterisation of nano functionalised coatings

Taking into account the results obtained, Ag5NPs suspension was selected as nano-additive to the formulation of the coatings. The proposed hydrolysis method allowed obtaining the sol-gel coating functionalised with Ag5NPs, a possible mechanism is proposed in the scheme of the figure 2 of supplementary material. Figure 3 of supplementary material depicted SEM micrographs, EDS spectra and x-ray mapping of obtained coatings. Firstly, sol-gel coating free paint presents an irregular surface with a partially homogeneous distribution of elements such as Ti, Ca and Mg. Also, EDS spectrum peaks for these elements are observed at 4.5, 4, and 1.2 keV, respectively (figure 3(A)). These elements are present in the chemical compounds used in the paint. However, SEM micrographs of both sol-gel coating and sol-gel coating + Ag5NPs over the paint show a homogeneous surface, possibly due to the presence of the coating. The sol-gel method affords high uniformity on the thin films with

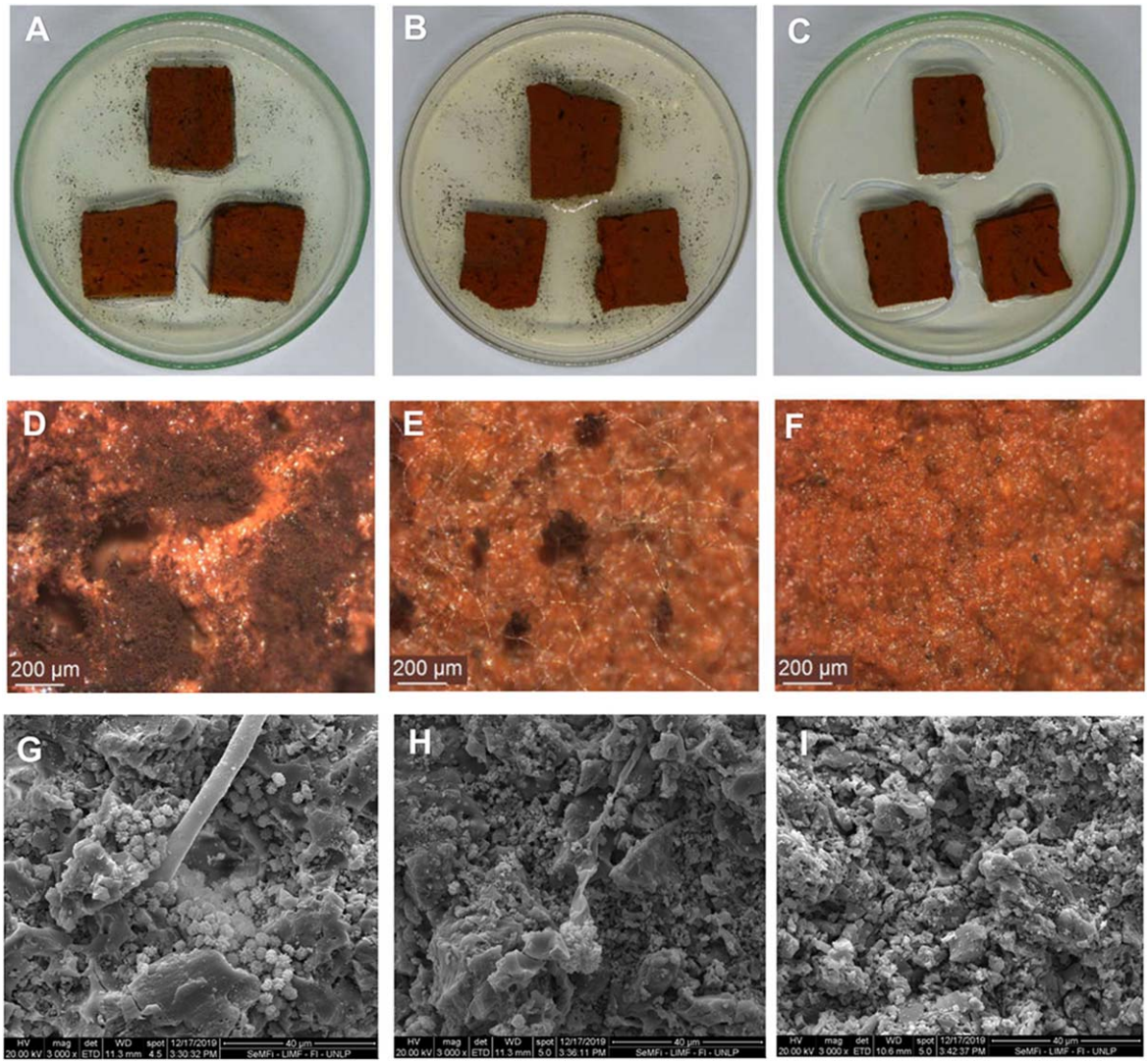

Figure 5. Fungal resistance test against *A. niger*, samples. (A), (D) and (G): control (brick free of sol-gel coating); (B), (E), and (H): brick with sol-gel coating; (C), (F), and (G): brick with sol-gel coating + Ag5NPs. (D)–(F) were obtained from stereoscopic microscope (80×), (G)–(I) SEM micrographs (3000×), $t = 30$ days.

different substrate combinations. If the surface on which the sol-gel is deposited is hydrophilic, it is chemically activated, and the generated gel is fine enough, the drying after gelling is so fast that it can prevent shrinkage and fracture of the coating. This is a compact, homogeneous and adherent coating. Although elements such as Ti, Ca, and Mg were also detected, the EDS spectrum detected N and Si at 0.4 and 1.7 keV (figures 3(B) and (C)). These elements are part of the AMEO chemical structure part of the aminosilane used [37]. The EDS spectrum of the sample with sol-gel coating + Ag5NPs over the paint does not show the characteristic Ag peak at 3 keV, as expected. This does not mean that the sample does not have Ag, simply that the concentration of this element is below the detection limit of the equipment (0.1 wt%).

Figure 4 of supplementary material depicts photographic records from water droplets on samples and the corresponding contact angles. Both the coated and uncoated paints were hydrophilic since the contact angle had values between 10 and 90° (figures 4(A)–(C)). Therefore, the coating did not change the hydrophobicity/hydrophilicity characteristics of the acrylic paint. However, there was a change in this physicochemical characteristic when the bricks were covered (figures 4(D)–(F)) as contact angle increased from <10° (superhydrophilic) to higher than 90° (hydrophobic).

3.4. Fungal resistance test of nano functionalised coatings

Table 1 illustrates the classification of fungal growth on the samples studied. The uncoated samples had heavy growth (60%–100%), except in the case of *P. commune* which had moderate growth on acrylic paint. On the samples coated with AMEO, growth similar to that described above was observed, although it was moderate (30%–60%) in *L. theobromae*. However, there was no fungal growth on the samples when they were coated with AMEO + Ag5NPs, except when *A. niger* and *P. commune* were inoculated on coated acrylic paint and brick, respectively. In this case, greater growth of *A. niger* was observed. In the case of the sol-gel + Ag5NP coating on

the paint, the hydrophilic surface would be more susceptible to colonisation by filamentous fungi due to its affinity for these types of substrates [38]. However, lower fungal growth is shown due to the presence of Ag5NPs. The antifungal activity of brick with sol-gel coating + Ag5NPs may then be due to the presence of NPs retained in the silane matrix and to the hydrophobicity surface [29].

Figure 4 depicted the resistance test with the samples with the sol-gel coating on the paint against *P. commune*. Both in the paint without and with the sol-gel coating, vegetative and reproductive mycelia were observed on the culture medium and on the samples (figures 4(A), (B), (D) and (E)). Instead, when this strain was inoculated in sol-gel coating + Ag5NPs over the paint, the mycelium grew only in the culture medium and not on the sample (figures 4(C) and (F)). This evidence shows that the antifungal activity of the coating is related to the presence of Ag5NPs. Figure 5 provides resistance test against *A. niger* on the samples of bricks. In this case, when the strain was inoculated in brick free of sol-gel coating (figures 5(A), (D) and (G)) and brick with sol-gel coating (figures 5(B), (E) and (H)), mycelial growth was observed. SEM images of these samples show conidia free and abundant, although to a lesser extent when the brick was covered with AMEO. Finally, *A. niger* was not able to colonise the bricks with sol-gel + Ag5NP coating (figures 5(C), (F) and (I)). In this case, it was also confirmed that the antifungal activity of the coating would be effective due to the presence of Ag5NP and the hydrophobicity that they provide to the material. To our knowledge, this is the first report of functionalised coating with AgNP synthesised from *C. spinosa* tannin for the protection of acrylic paints and bricks in the control of materials fungal deterioration.

4. Conclusions

Through phytogenic synthesis, using *Caesalpinia spinosa* tannin, the efficient obtainment of silver and Copper oxide NPs was possible. The silver NPs obtained with 500 ppm aqueous solution of tara tannin (Ag5NPs) showed lower average size (12 nm) and higher antifungal activity against *A. niger*, *P. commune* and *L. theobromae* compared to the other NPs obtained. The internalisation of Ag5NPs in a protective sol-gel antifungal coating applied on bricks and acrylic paint films with a low silver concentration (10.8 mg/100 ml^{-1} of the coating) was a novel result. Therefore, the method reported a low-cost and eco-friendly bioactive system with more than one possible application.

Acknowledgments

Authors are thankful for the essential support of Consejo Nacional de Investigaciones Científicas y Técnicas (CONICET), Comisión de Investigaciones Científicas de la provincia de Buenos Aires (CICPBA), Agencia Nacional de Promoción Científica y Tecnológica (ANPCyT) and Universidad Nacional de La Plata (UNLP). They also thank the technical support of the Ing. Pablo Bellotti, Ing. Pablo Seré and Lic. Claudio Cerruti.

References

[1] Gallego-Cartagena E, Morillas H, Maguregui M, Patiño-Camelo K, Marcaida I, Morgado-Gamero W, Silva L F O and Madariaga J M 2020 *Int. Biodeterior. Biodegradation* **147** 104874
[2] Kakakhel M A, Wu F, Gu J-D, Feng H, Shah K and Wang W 2019 *Int. Biodeterior. Biodegradation* **143** 104721
[3] Coutinho M L, Miller A Z and Macedo M F 2015 *J. Cult. Herit.* **16** 759
[4] Barberia-Roque L, Gámez-Espinosa E, Viera M and Bellotti N 2019 *Int. Biodeterior. Biodegradation* **141** 52
[5] Nasrollahzadeh M, Sajjadi M, Sajadi S M and Issaabadi Z 2019 *An Introduction to Green Nanotechnology* 1st edn (New York: Academic) vol 28, p 145
[6] Corsi I *et al* 2018 *Ecotoxicol. Environ. Saf.* **154** 237
[7] Wang Z, Li Q, Xu L, Ma J, Wang Y, Wei B, Wu W and Liu S 2020 *Ecotoxicol. Environ. Saf.* **196** 110487
[8] Sharma D, Kanchi S and Bisetty K 2019 *Arab. J. Chem.* **12** 3576
[9] Ahmed S, Ahmad M, Swami B L and Ikram S 2016 *J. Adv. Res.* **7** 17
[10] Kumar I, Mondal M and Sakthivel N 2019 *Green Synthesis, Characterization and Applications of Nanoparticles* (Amsterdam: Elsevier) p 37
[11] Pethakamsetty L, Kothapenta K, Nammi H R, Ruddaraju L K, Kollu P, Yoon S G and Pammi S V N 2017 *J. Environ. Sci.* **55** 157
[12] Bellotti N, Del Amo B and Romagnoli R 2012 *Prog. Org. Coatings* **74** 411
[13] Ping L, Pizzi A, Guo Z D and Brosse N 2012 *Ind. Crops Prod.* **40** 13
[14] Teng B, Hayasaka Y, Smith P A and Bindon K A 2019 *J. Agric. Food Chem.* **67** 8938
[15] Pinela J, Prieto M A, Pereira E, Jabeur I, Barreiro M F, Barros L and Ferreira I C F R 2019 *Food Chem.* **275** 309
[16] Braga W L M, Roberto J A, Vaz C, Samanamud G R L, Loures C C A, França A B, Lofrano R C Z, Naves L L R, José Henrique de Freitas Gomes J H and Naves F L 2018 *J. Environ. Chem. Eng.* **6** 4310
[17] Guo L, Qiang T, Ma Y, Wang K and Du K 2020 *Ind. Crops Prod.* **149** 112360
[18] Cordero I, Jiménez M D, Delgado J A, Villegas L and Balaguer L 2016 *For. Ecol. Manage.* **377** 71
[19] Spennati F, Mora M, Tigini V, La China S, Di Gregorio S, Gabriel D and Munz G 2019 *J. Environ. Manage.* **231** 137
[20] Badhani B, Sharma N and Kakkar R 2015 *RSC Adv.* **5** 27540
[21] Odeniyi M A, Okumah V C, Adebayo-Tayo B C and Odeniyi O A 2020 *Sustain. Chem. Pharm.* **15** 100197
[22] Valsalam S, Agastian P, Arasu M V, Al-Dhabi N A, Ghilan A K M, Kaviyarasu K, Ravindran B, Chang S W and Arokiyaraj S 2019 *J. Photochem. Photobiol. B Biol.* **191** 65
[23] Kaviyarasu K, Geetha N, Kanimozhi K, Maria Magdalane C, Sivaranjani S, Ayeshamariam A, Kennedy J and Maaza M 2017 *Mater. Sci. Eng.* C **74** 325
[24] Kaviyarasu K, Kanimozhi K, Matinise N, Maria Magdalane C, Mola G T, Kennedy J and Maaza M 2017 *Mater. Sci. Eng.* C **76** 1012
[25] Deyá C and Bellotti N 2017 *Adv. Nat. Sci. Nanosci. Nanotechnol.* **8** 025005
[26] Chen A J *et al* 2017 *Stud. Mycol.* **88** 37

[27] Schoch C L, Seifert K A, Huhndorf S, Robert V, Spouge J L, Levesque C A, Chen W and Fungal Barcoding Consortium 2012 *Proc. Natl. Acad. Sci.* **109** 6241
[28] Fernández M A, Barberia Roque L, Gámez Espinosa E, Deyá C and Bellotti N 2020 *Appl. Clay Sci.* **184** 105369
[29] Gámez-Espinosa E, Barberia-Roque L, Obidi O F, Deyá C and Bellotti N 2020 *Adv. Nat. Sci. Nanosci. Nanotechnol.* **11** 015019
[30] Koch K and Barthlott W 2009 *Philos. Trans. R. Soc. A Math. Phys. Eng. Sci.* **367** 1487
[31] Simões M F, Santos C and Lima N 2013 *Microsc. Microanal.* **19** 1151
[32] Kerour A, Boudjadar S, Bourzami R and Allouche B 2018 *J. Solid State Chem.* **263** 79
[33] Shah Z *et al* 2020 *Mater. Sci. Eng.* C **111** 110829
[34] Singh K S, Majik M S and Tilvi S 2014 *Analysis of Marine Samples in Search of Bioactive Compounds* (Amsterdam: Elsevier) p 115
[35] Zmozinski A V, Peres R S, Freiberger K, Ferreira C A, Tamborim S M M and Azambuja D S 2018 *Prog. Org. Coatings* **121** 23
[36] Shen T, Wang Q, Li C, Zhou B, Li Y and Liu Y 2020 *J. Hazard. Mater.* **388** 122063
[37] Roushani M, Rahmati Z, Farokhi S, Hoseini S J and Fath R H 2020 *Mater. Sci. Eng.* C **108** 110388
[38] Linder M B, Szilvay G R, Nakari-Setälä T and Penttilä M E 2005 *FEMS Microbiol. Rev.* **29** 877